Journal of Medicinal Chemistry

ARTICLE

pubs.acs.org/jmc

SAR by Interligand Nuclear Overhauser Effects (ILOEs) Based Discovery of Acylsulfonamide Compounds Active against Bcl-x_L and Mcl-1

Michele F. Rega, Bainan Wu, Jun Wei, Ziming Zhang, Jason F. Cellitti, and Maurizio Pellecchia*

Sanford−Burnham Medical Research Institute, 10901 North Torrey Pines Road, La Jolla, California 92037, United States

Supporting Information

ABSTRACT: Overexpression of antiapoptotic members of the Bcl-2 family proteins, such as Bcl-x_L and Mfl-1, has been shown to be involved in resistance to chemotherapeutic drugs in many forms of cancers. Recent efforts from the Abbott Laboratories resulted in the development of the acylsulfonamide compound and clinical candidate that targets selectively Bcl-2, Bcl-x_L, and Bcl-w while it is not active against Mcl-1 and Bfl-1. However, early clinical and preclinical studies suggest that pan-Bcl-2 antagonists, targeting simultaneously Mcl-1, Bcl-xL, and possibly all other four antiapoptotic Bcl-2 proteins, may result in more efficacious drugs. Here, following an NMR fragment-based approach, SAR by ILOEs, we report on compounds that exhibit nanomolar affinities for both Bcl-x_L and Mcl-1 in vitro. We believe that these molecules can be used as useful starting point for the development of novel Bcl-2 antagonists, in particular targeting Mcl-1.

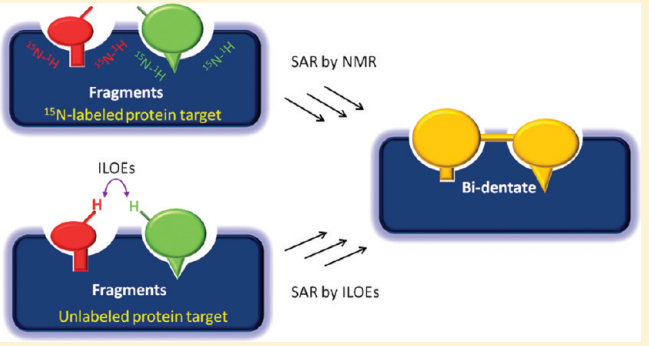

INTRODUCTION

In the past few years, an increased number of chemical fragment-based approaches to inhibitor design and drug discovery have been successfully applied to unconventional and challenging drug target such as those involving protein−protein interactions.[1−5] One of the first and most successful fragment-based method is the SAR by NMR that is directed at linking two different molecules of modest affinity into a single molecule with higher affinity (Figure 1A). The approach is based on first and second site NMR screening using uniformly ^{15}N-labeled protein and [^{15}N,^{1}H]-HSQC chemical perturbation studies. Subsequent structure determination of the ternary complex by NMR is obtained prior to attempting the chemical synthesis of linked compounds (Figure 1).[1]

Recently, compound **3** (Figure 1) was developed from the Abbott Laboratories[6] using such an approach. In particular, application of the HSQC NMR-based screening yielded an initial fluoro-biaryl acid (**1**) with an affinity (K_D) of 300 μM for Bcl-x_L. Following the SAR by NMR approach, a second-site ligand was identified in a tetrahydronaphthalen-1-ol (**2**) with an affinity (K_D) of 4300 μM for the protein (Figure 1).[6] From NMR-based structural studies and iterative steps of parallel synthesis, a potent ligand which binds to Bcl-x_L with an IC_{50} value of 36 nM in a fluorescence polarization displacement assay was finally obtained (**3**).[6] Further optimizations of compound **3** led to a compound inhibiting Bcl-2, Bcl-x_L, and Bcl-w.[7] The molecule markedly increased the response to radiation as well as to multiple chemotherapy agents in vitro and showed good activity as a single agent in two small cell lung cancer xenograft models.[7] A closely related second-generation compound Navitoclax (ABT-263) is currently undergoing clinical evaluations (www.cancer.gov). Unfortunately, consistent with the low affinity of this compound for Mcl-1, multiple reports have suggested that high basal levels of Mcl-1 expression are associated with resistance to this compound.[8−11] Along these lines of research, we also have recently described a powerful fragment-based NMR method, named SAR by ILOEs (*s*tructure *a*ctivity *r*elationships by *inter*ligand nuclear *O*verhauser *e*ffect),[12,13] which led to the identification of high affinity ligands against Bid, a pro-apoptotic member of the Bcl-2 family of proteins.[12−14] Unlike the SAR by NMR, the NMR-based screen is set up to directly identify a pair of ligands from a diverse library of fragments by detecting protein-mediated ligand−ligand NOEs (ILOEs), which are then used directly to guide the synthesis of bidentate ligands from the individual fragments (Figure 1).[1,15] Hence, the SAR by ILOEs overcome two major bottle necks in the SAR by NMR approach: protein labeling and resonance assignments, HSQC-based NMR screens and structure determination of the ternary complex, both labor intensive tasks that are limited to relatively small (<25 kDa)

Received: March 29, 2011
Published: July 28, 2011

dx.doi.org/10.1021/jm200826s | *J. Med. Chem.* 2011, 54, 6000–6013

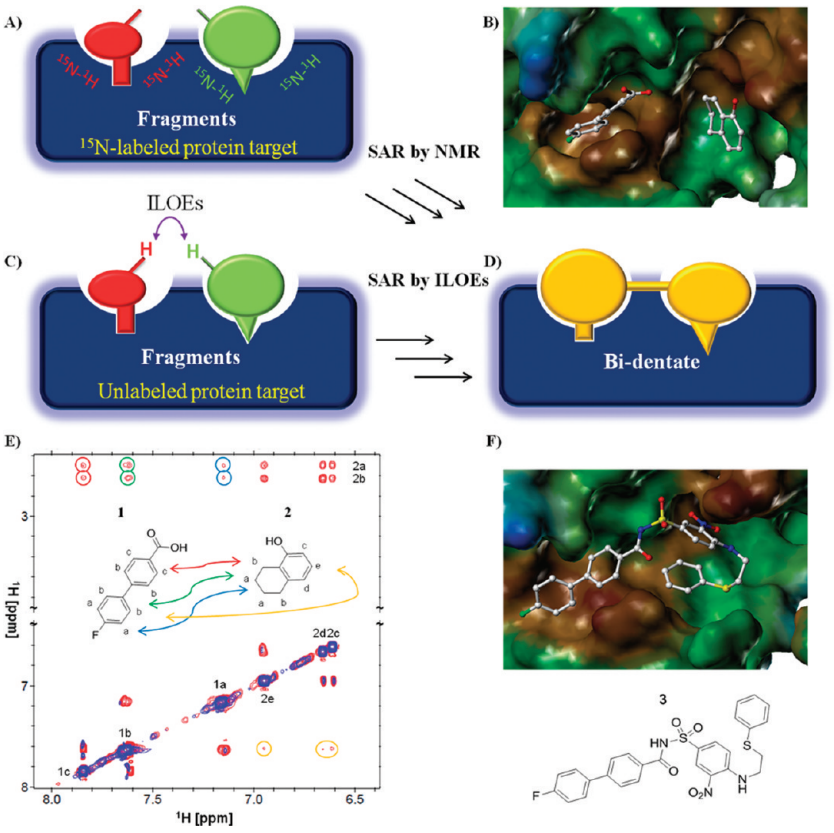

Figure 1. Comparison between the SAR by NMR and SAR by ILOEs approach as applied to Bcl-x_L. (A) Schematic representation of the SAR by NMR approach as applied to Bcl-xL. (B) NMR structures of fragment **1** and **2** in complex with Bcl-x_L (PDB ID 1YSG). The final bidentate (D), compound **3**, in complex with Bcl-x_L (PDB ID 1YSI) is reported in (F)); the protein color code is according to the lipophilic potential. (C) schematically illustrates the SAR by ILOEs approach. When applied to the same Bcl-xL binding fragments discovered via the SAR by NMR approach, Bcl-x_L mediated ILOEs between these fragments are detected (E). The spectra in (E) represent superposition of two 2D [^{1}H, ^{1}H] NOESY spectra of the ligands (250 μM each) in the presence of a substoichiometric amount of Bcl-x_L (10 μM) and in presence (blue) and absence (red) of a saturating concentration (50 μM) of a Bak derived BH3 peptide. Circles indicate ILOEs that are labeled with arrows of corresponding colors of the chemical structures of the fragments.

and highly soluble protein targets. Here, we first demonstrate that the SAR by ILOE could have led to similar scaffolds identified by the SAR by NMR for Bcl-x_L and, subsequently, we report on the identification of novel scaffolds that lead to small molecule bidentate compounds active against both Bcl-x_L and Mcl-1 with nanomolar affinities.

RESULTS AND DISCUSSION

The screening strategies used relies on the detection of protein mediated (often referred to as "transferred effect") ligand−ligand NOEs (ILOEs).[15−17] Small molecules tumble rapidly in solution, and the dominant ^{1}H relaxation mechanisms, during a NOESY-type experiment, lead to weak positive NOEs (cross peaks have opposite sign than diagonal peaks, short relaxation time). In contrast, when a small molecule is bound transiently to a target protein, it assumes its long correlation time. In the case of a fast exchange between free and bound state (weak binders in the μM to mM range), this translates into very strong negative NOEs (very strong positive cross-peaks in a NOESY-type experiment). The use of 2D [^{1}H,^{1}H]-NOESY spectra[18] can be used as tool for the detection of pairs of small-molecular binders. That is, if two ligands bind simultaneously in adjacent sites on the protein surface, strong negative ligand−ligand NOEs (ILOEs) will also observed.[19−23] Compounds that display these protein-mediated ligand−ligand interactions can then serve to design covalently linked compounds with increased affinity (Figure 2A).[19−23] A 500 compound fragment library was selected including low molecular weight compounds (MW < 300) representing a selection of drug-like substructures[24] and that are amenable to subsequent chemistry.

As recently reported,[14] we further validate here that the detection of such interactions can be accomplished also in complex mixtures where deconvolution can be easily achieved aided by the 1D ^{1}H NMR spectra of individual compounds. Hence, we prepared several mixtures of compounds from our library of scaffolds (0.250−1 mM each) and tested them in presence of 10 μM Bcl-x_L. Typical trNOESY spectra were measured with 8 or 16 transients per increment with mixing times of 300−800 ms to maximize the detection of trNOEs and ILOEs.[20] The compounds were prepared in mixtures of 10−50, thus allowing the collection of the spectra for our 500 fragments library in a few days. Analysis of the data and subsequent deconvolution of the spectra allowed us to identify and discard weak ligands by means of positive trNOEs cross peaks. Similarly, compounds that bind Bcl-x_L in close proximity (less than 5−6 Å) were identified by detecting intermolecular NOEs[19−23,25] and subsequently used as building blocks for producing linked compounds. Finally, to eliminate compounds that may give rise to ILOEs due to nonspecific interactions, displacement assays in

dx.doi.org/10.1021/jm200826s |J. Med. Chem. 2011, 54, 6000–6013

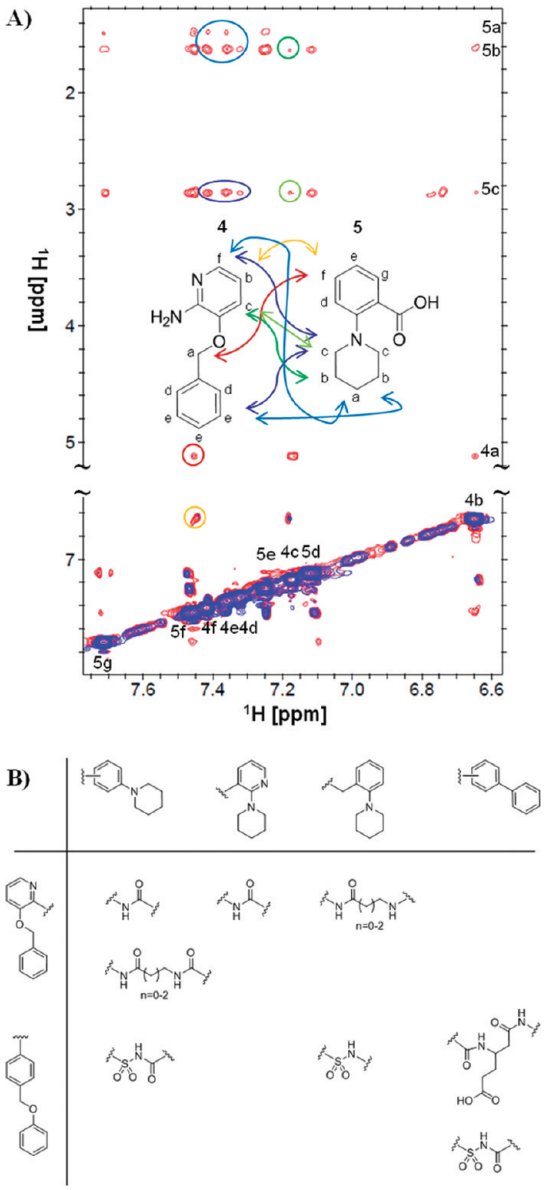

Figure 2. Application of SAR by ILOEs approach to Bcl-x_L. (A) Superposition of a portion of the 2D [^{1}H, ^{1}H]-NOESY spectrum of respectively fragment **4** (250 μM) and fragment **5** (250 μM) all in presence of Bcl-x_L 10 μM, in the absence (red spectrum), and presence (blue spectrum) of the BH3 peptide from BAK (50 μM). Circles represent ILOEs cross-peaks between the two molecules. (B) Chemical structures of the resulting combinatorial linking strategy.

which a known binder such as a BH3 peptide is included in the NMR sample are collected. If the pair of compounds binds in the BH3 binding groove, addition of saturating amount of a BH3 peptide should result in the suppression of ILOEs in the NOESY spectra (Figure 1E, blue spectra).

As proof-of-concept, the experiments were conducted first on the initial pair of fragments that were recognized to bind to Bcl-x_L by Petros et al. using the SAR by NMR approach[6] (compounds **1** and **2**) that led to the synthesis of compound **3** (Figure 1F). For this binder, the NMR structure in complex with Bcl-x_L (PDB ID 1YSI, Figure 1) was also obtained. As depicted in the part E of Figure 1, strong negative Bcl-x_L-mediated ILOEs between methylene hydrogen atoms of fragment **2** and hydrogen atoms

Table 1. Chemical Structures and FPA Displacement Data (IC_{50} Values) against Bcl-x_L and Mcl-1[a]

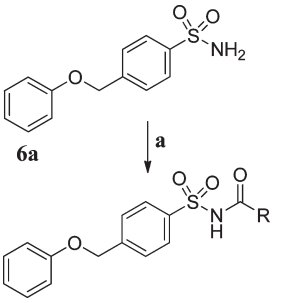

R	ID	IC_{50} (μM) Bcl-x_L	IC_{50} (μM) Mcl-1
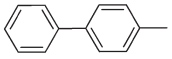	**7a**	16.77 ± 0.12	43.22 ± 0.01
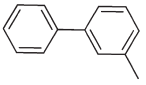	**7b**	15.08 ± 0.06	25.38 ± 0.02
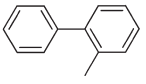	**7c**	42.72 ± 0.26	>1000

[a] Reagents and conditions: (a) [1,1′-biphenyl] carboxylic acids, EDC, DMAP, CH_2Cl_2, rt, 24 h.

of the biaryl acid **1** can be easily identified. These ILOEs and most of the intramolecular NOEs are largely eliminated by the addition of a BH3 peptide of Bak (G-G-G-Q-V-G-RQ-L-A-I-I-G-D-D-I-N-R) to the NMR sample (Figure 1E). Similarly, the NMR screen of our library led to an additional pair of fragments (compound **4** and **5**) that was selected among the library based on Bcl-x_L-mediated ILOEs (Figure 2). Fragments **4** and **5** were found to bind to Bcl-x_L with an affinity (K_D) of 691.8 ± 205.50 and 378.4 ± 75.70 μM, respectively, via an NMR-based titration.[26] Again, the ILOEs disappear in presence of a BH3 peptide from Bak (Figure 2A). From the 2D-NOESY spectra reported in Figure 2, it is possible to identify strong negative ILOEs between methylene hydrogens of fragment **5** and the hydrogen atoms of the 3-(benzyloxy)pyridin-2-amine **4**, in analogy to those reported in Figure 1E. In addition, equally strong ILOEs between the methylene hydrogen atoms of fragment **4** and hydrogen atoms of the 2-(piperidin-1-yl)benzoic acid **5** can be observed (Figure 2A).

To prioritize synthetic efforts while proposing an appropriate linking strategy of the two fragments, we adopted in silico docking by using Gold.[27,28] Several types of linkers were proposed to connect fragment **4** to fragment **5** (Figure 2). Among the synthesized compounds listed in Figure 2B, the 4-(phenoxymethyl)-benzene and [1,1′-biphenyl] linked with an acylsulfonamide linker, resulting in compounds **7a**, **7b**, and **7c**, were found to bind to Bcl-x_L with IC_{50} values of 16.8, 15.1, and 42.7 μM, respectively, as measured by FP assay (Table 1). Other linkers led to compounds with much lower affinity for Bcl-x_L, with the exception of the 3-aminohexanedioic acid linker, which resulted in compounds with micromolar affinity. Because the acylsulfonamide linker has already been reported in the clinical

dx.doi.org/10.1021/jm200826s |J. Med. Chem. 2011, 54, 6000–6013

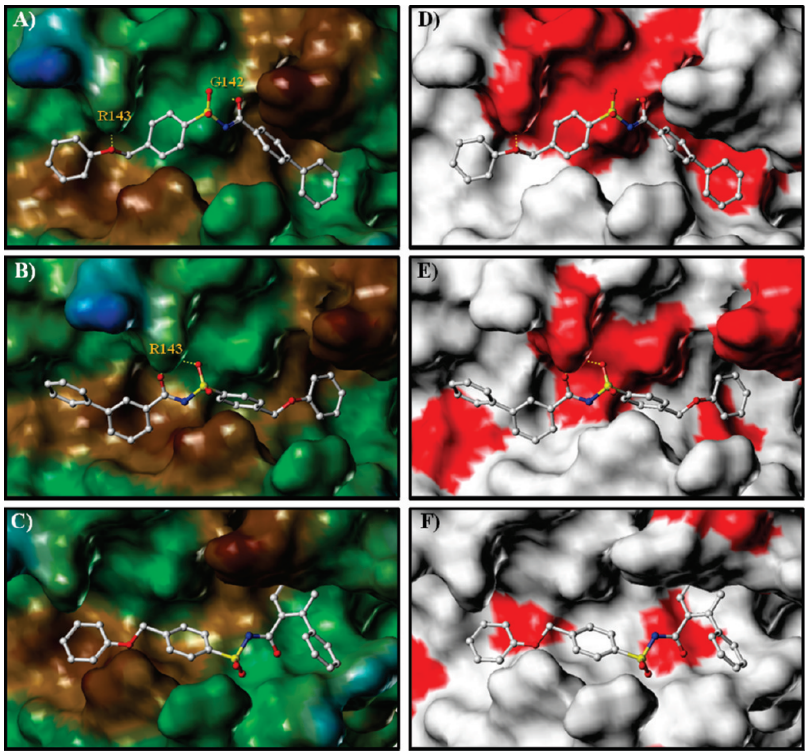

Figure 3. Molecular docking studies with Bcl-x_L. The docked structure of compounds **7a**, **7b**, and **7c** are reported in (A) and (D), (B) and (E), and (C) and (F) respectively in to the BH3-binding pocket of Bcl-x_L (PDB ID 1YSI). The MOLCAD protein surface is colored according to the lipophilic potential in (A), (B), and (C), and according to chemical shift perturbations (red, residues with $\Delta\delta \geq 0.1$ ppm upon complexation) in (D), (E), and (F).

candidate from Abbott,[7] we decided to focus on this moiety for our optimizations. The docking predictions show the compounds interacting with both sites of the hydrophobic groove of Bcl-x_L (Figure 3). Compound **7a** can deeply occupy mainly the second site of the binding pocket with the acylsulfonamide linker involved in a H-bond with residue G142 and the 4--(phenoxymethyl)-benzene moiety involved in a H-bond with residue R143 (Figure 3a), similarly to what was found for compound **3** (PDB ID 1YSI, Figure 1F). Differently, compound **7b** projects the biphenyl moiety deeply into the first site of the binding pocket and the acylsulfonamide linker, involved in a H-bond with residue R143, appear to sit just on top of the bridge connecting the two sites (Figure 3B). On the contrary, the binding of compound **7c** is predicted to take place prevalently into the second binding subpocket with no H-bonds apparently involved with the protein (Figure 3C).

These observations could be used to explain the trend of activity of these compounds reported in Table 1. To better rationalize the experimental data and successively uncover areas for further gains in affinity, we have used [^{15}N, ^{1}H]-HSQC NMR experiments in the presence and absence of added compounds (Supporting Information). On the basis of the available resonance assignments, we have also mapped chemical shift changes induced by the compounds into the NMR structure of Bcl-x_L in complex with compound **3** (PDB ID 1YSI). This data demonstrates that most of the resonances that are significantly affected by the compound are indeed located in the BH3 binding pocket of Bcl-x_L (Figure 3). When compared with the predicted docked geometries of the compounds (Figure 3A−C), the mapping data also reveal a fairly good agreement (Figure 3D−F). Interestingly, in agreement with the predicted geometries, when the same fragments are linked together trough the ortho, meta, or para position of the biaryl acid, the resulting compounds induce a rather different chemical shift perturbation.

Next we evaluated the activity of the designed Bcl-x_L binders against Mcl-1 in a similar FP assay (Table 1). Modest activities were detected for compounds **7a** and **7b**, with IC_{50} values of 43.2 and 25.4 μM, respectively, while compound **7c** binds to Mcl-1, with IC_{50} value greater than 1000 μM. Comparison of the predicted binding geometries of the compounds into the Mcl-1 binding pocket and the mapped chemical shift changes induced into the Mcl-1 structure (PDB ID 2NL9, Table 1) in the presence of added compounds suggests that while compounds **7a** and **7b** can similarly interact in the hydrophobic groove of the protein (Figure 4D,E), compound **7c** does not have a good fit for each subpockets as confirmed by experimental data (Figure 4F). On the basis of these initial results, compounds **7a** and **7b** were selected for further optimizations to improve potency against both targets. Analysis of the docked structures of compound **7a** into both targets binding pockets (Figures 3A and 4A) suggests that the insertion of substituent on the second benzyl ring of the biphenyl moiety may uncover unoccupied regions in the first and second sites of Bcl-x_L and Mcl-1 binding grooves, respectively. Table 2 shows, in fact, that when a fluorine or chlorine atom is added on the para position of compound **7a**, the potency of the resulting compounds, **8** and **9**, increases significantly for both targets. Addition of chlorine atoms in 3 and 5 position of compound **7a** results in compound **10** with approximately 4-fold and 17-fold improvement in potency over the original biphenyl for Bcl-x_L and Mcl-1, respectively, thus confirming our assumptions.

dx.doi.org/10.1021/jm200826s |*J. Med. Chem.* 2011, 54, 6000–6013

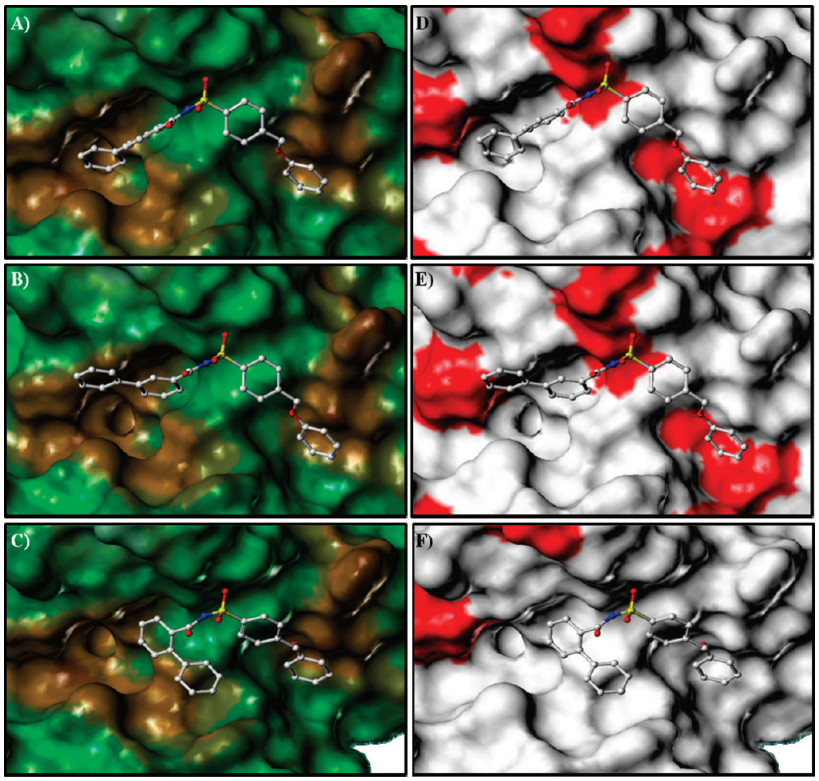

Figure 4. Molecular docking studies with Mcl-1. The docked structure of compounds **7a**, **7b**, and **7c** are reported in (A) and (D), (B) and (E), and (C) and (F) respectively in to the BH3-binding pocket of Mcl-1 (PDB ID 2NL9). The MOLCAD protein surface is colored according to the lipophilic potential in (A), (B), and (C), and according to chemical shift perturbations (red, residues with $\Delta\delta \geq 0.05$ ppm upon complexation) in (D), (E), and (F).

Table 2. Influence of Various Substituents on the Second Benzyl Ring of the Biphenyl Moiety of Compound 7a for Binding to Bcl-x_L and Mcl-1

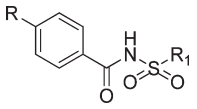

R	R_1	ID	IC_{50} (μM) Bcl-x_L	IC_{50} (μM) Mcl-1
	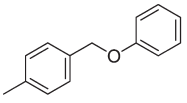	**7a**	16.77 ± 0.12	43.22 ± 0.01
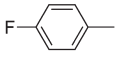	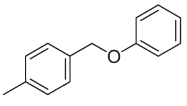	**8**	9.37 ± 0.05	16.63 ± 0.02
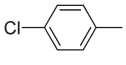	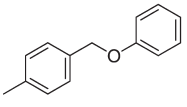	**9**	3.79 ± 0.03	7.26 ± 0.03
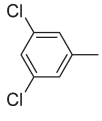	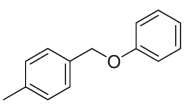	**10**	4.14 ± 0.03	2.51 ± 0.07

To prove the relevance of the 4-(phenoxymethyl)-benzene moiety of compound **7a**, additional compounds were synthesized and tested for binding to both proteins (Table 3). The shortening of the 4-(phenoxymethyl)-benzene moiety by one methylene unit results in compounds with decreased affinities to Bcl-x_L (compare compounds **7a**, **8**, and **10** in Table 2 to compounds **11**, **12**, and **13** in Table 3). The affinity to Mcl-1 of compounds **12** and **13** (Table 3) is comparable to that of compounds **8** and **10** (Table 2), while compound **11** is approximately 14-fold more potent compared to compound **7a** (Table 1). These results indicate that the affinity of the original hit, compound **7a**, to Bcl-x_L and Mcl-1 can be progressively increased by introducing bulky substituents on the second benzyl ring of the biphenyl moiety. On the other hand, when the 4-(phenoxymethyl)-benzene moiety of compound **7a** is replaced with 4-(phenoxy)-benzene, an opposite trend on the affinity can be observed (Table 3). A similar trend of activity, except for compound **11**, is obtained for compounds binding to Mcl-1. Ultimately, when the 4-(phenoxymethyl)-benzene moiety of compound **7a** is replaced with 1-(benzyloxy)-4-methylbenzene, retaining exactly the length of compound **7a** as in compound **13a**, the affinity versus Bcl-x_L can be increased 15-fold in potency over that of compound **13** (Table 3). Interestingly, when the two fragment moieties are linked together with a reversed sulfonamide linker (compound **14**, Table 3), the affinity to both proteins decreases several orders of magnitude. Correspondingly, in order to improve the potency of compound **7b** to Bcl-x_L and to Mcl-1, a small library of analogues was generated. Once again, as reported in Table 4, the presence of substituents on the second benzyl ring

Table 3. Relevance of the 4-(Phenoxymethyl)-benzene Moiety of Compound 7a for the Inhibition of Bcl-x_L and Mcl-1 Binding to a BH3 Peptide

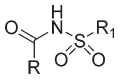

R	R_1	ID	IC_{50} (μM) Bcl-x_L	IC_{50} (μM) Mcl-1
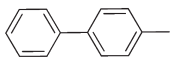	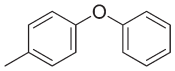	**11**	28.03 ± 0.04	3.56 ± 0.03
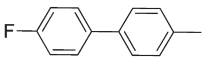	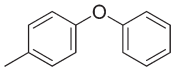	**12**	33.52 ± 0.05	17.79 ± 0.03
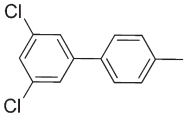	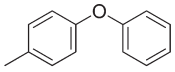	**13**	49.51 ± 1.2	5.08 ± 0.02
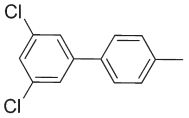	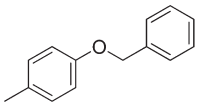	**13a**	3.19 ± 0.02	6.30 ± 0.03
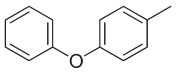	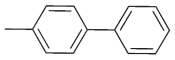	**14**	161.3 ± 2.68	>1000

of the biphenyl moiety of compound **7b** confirmed our hypothesis. Addition of 4-trifluoro-methyl or 2,4-dichloro or 3,4-dichloro substituents lead to compounds **15**, **17**, and **18** with increased potency to Bcl-x_L and Mcl-1, respectively (Table 4).

When the two chlorine atoms are added in positions 3 and 5 on the second benzyl ring of the biphenyl moiety of compound **7b**, the resulting compound, **16**, binds to Bcl-x_L and Mcl-1 with IC_{50} values of 0.3 and 5.1 μM, respectively (Table 4). This represents a 50-fold improvement in potency to Bcl-x_L but just a 5-fold improvement in potency to Mcl-1 over the original compound **7b**. When the 4-(phenoxymethyl)-benzene moiety of compound **7b** is replaced with 1-(benzyloxy)-4-methylbenzene, compound **16a**, a greater than 80-fold and 115-fold improvements in potency to Bcl-x_L and a Mcl-1 respectively over the original compound **7b** are finally obtained.

To further investigate the role of the 4-(phenoxymethyl)-benzene moiety of compound **7b** for binding to Bcl-x_L and Mcl-1, additional compounds were synthesized and tested (Table 5). Compound **19** binds to Bcl-x_L almost 1-fold in potency weaker than compound **7b** while the binding to Mcl-1 increases 8-fold in potency, as previously registered. Compound **20** shows the same affinity as compound **16** to Mcl-1 although a significant drop in potency, 8-fold, to Bcl-x_L is registered. Compound **24** binds to Bcl-x_L and Mcl-1 with same affinity and, finally, when the 4-(phenoxy)-benzene moiety replaces the 4-(phenoxymethyl)-benzene moiety of compounds **17** and **18**, generating compounds **22** and **23**, the binding affinities increase 5- and 4-fold to Bcl-x_L respectively and only 2-fold to Mcl-1 for both compounds. Analysis of the compounds listed in Tables 2 and 3 shows that the binding affinities of the initial bidentate compounds **7a** to Bcl-x_L and Mcl-1 can be modestly improved by adding substituents on the second benzyl ring of the biphenyl moiety and when the 4-(phenoxymethyl)-benzene moiety is replaced with the 1-(benzyloxy)-4-methylbenzene. Differently, the binding affinity of compounds **7b** derivatives to Bcl-x_L and Mcl-1 is more susceptible to derivatizations as reported in Table 4 and 5. Hence, we selected compound **23** as hit to conduct the final round of optimization. Table 6 shows that when the 4-(phenoxymethyl)-benzene moiety of compound **23** is replaced as in compounds **26** and **27**, a drop in potency versus both targets is registered while compound **28** retains almost the same affinity of compound **23** to both proteins. Differently, when the 1-(cyclohexylmethoxy)-4-methylbenzene replaces the 4-(phenoxymethyl)-benzene moiety of compound **23**, compound **29** binds to Bcl-x_L and Mcl-1 with IC_{50} values of 0.16 and 0.62 μM, respectively (Table 6). Addition of various substituents on the second benzyl ring of the 4-(phenoxymethyl)-benzene moiety of compound **23** resulted in compounds with very similar binding affinities versus both targets (compounds **30**−**34**, Table 6). Finally, when 1-ethoxy-4-(*p*-tolyloxy)benzene is used to replace the 4-(phenoxymethyl)-benzene moiety, the resulting compound **35**, Table 6, binds to Bcl-x_L and Mcl-1, with IC_{50} values of 0.086 and 0.14 μM, respectively. This represents a 175-fold improvement in potency to Bcl-x_L and 181-fold improvement in potency to Mcl-1 over the original compound **7b**.

dx.doi.org/10.1021/jm200826s |*J. Med. Chem.* 2011, 54, 6000–6013

Table 4. Influence of Various Substituents on the Second Benzyl Ring of the Biphenyl Moiety of Compound 7b for the Inhibition of Bcl-x_L and Mcl-1 Binding to a BH3 Peptide

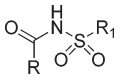

R	R_1	ID	IC_{50} (μM) Bcl-x_L	IC_{50} (μM) Mcl-1
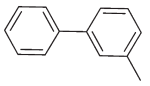	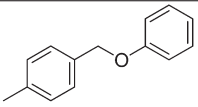	**7b**	15.08 ± 0.06	25.38 ± 0.02
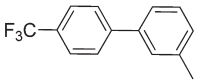	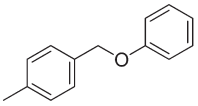	**15**	6.20 ± 0.06	8.37 ± 0.01
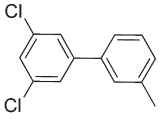	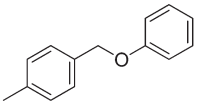	**16**	0.31 ± 0.43	7.57 ± 0.09
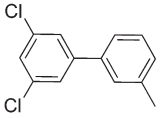	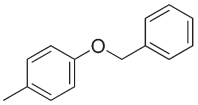	**16a**	0.18 ± 0.10	0.22 ± 0.06
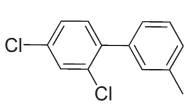	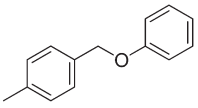	**17**	9.98 ± 0.03	8.69 ± 0.01
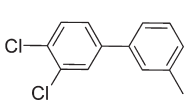	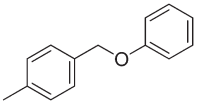	**18**	7.15 ± 0.02	5.76 ± 0.02

CONCLUSIONS

We have identified low-affinity fragments for the antiapoptotic protein Bcl-x_L through a powerful fragment-based NMR method, named SAR by ILOEs.[12−14] After initial systematic chemical linkage, the two fragments yielded a class of acylsulfonamide bidentate compounds with an affinity for Bcl-x_L and Mcl-1 in the mid-micromolar range. The binding mode predictions of these compounds to Bcl-x_L and Mcl-1, supported by NMR chemical shift mapping data, have been used to iterative synthesis of analogues with improved affinities to both targets, leading to compound **35** with nanomolar affinity for both Bcl-x_L and Mcl-1 (Figure 5). Since recent studies indicated that in most cancer types a strategy targeted to Mcl-1 inhibition, or combination of Bcl-x_L and Mcl-1 inhibition for certain solid tumors,[29] may prove to be more successful than therapies targeting only Bcl-2,[30] these data may provide a rationale and initial chemical matter that could be used to derive compounds that are more effective in targeting simultaneously Bcl-x_L and Mcl-1. Our manuscript also demonstrates the use of the SAR by ILOEs in targeting large protein surfaces such as those involved in protein−protein interactions.

EXPERIMENTAL SECTION

General Synthetic Procedures. Unless otherwise indicated, all reagents and anhydrous solvents (CH_2Cl_2, THF, diethyl ether, etc.) were obtained from commercial sources and used without purification. All reactions were performed in oven-dried glassware. All reactions involving air or moisture sensitive reagents were performed under a nitrogen atmosphere. Silica gel chromatography was performed using prepacked silica gel (RediSep), respectively. All final compounds were purified to >95% purity, as determined by a HPLC Breeze from Waters Co. using an Atlantis T3 3 μM 4.6 mm × 150 mm reverse phase column. ^{1}H NMR spectra were recorded on Bruker 600 MHz instruments. Chemical shifts are reported in ppm (δ) relative to ^{1}H (Me_4Si at 0.00 ppm). Coupling constant (J) are reported in Hz throughout. Mass spectral data were acquired on Shimadzu LCMS-2010EV for low resolution and on an Agilent ESI-TOF for high resolution.

General Solution Coupling. To a stirred solution of the appropriate acid (1.2 equiv) in CH_2Cl_2 10 mL, 4-(phenoxymethyl)benzenesulfonamide (1.0 equiv) was added, followed by *N*-(3-dimethylaminopropyl)-*N*′-ethyl-carbodiimide hydrochloride (1.2−2.0 equiv) and then DMAP (2.0 equiv). The solution was stirred at room temperature for 24−32 h and then diluted with saturated NH_4Cl. The layers were separated, and the aqueous layer was extracted with CH_2Cl_2. The combined organic layers were dried over $MgSO_4$ and concentrated under reduced pressure. The residue was purified by flash chromatography eluting with 10% MeOH in DCM to afford 70−90% of the final compound (Table 1).

***N*-((4-(Phenoxymethyl)phenyl)sulfonyl)-[1,1′-biphenyl]-4-carboxamide (7a).** Compound **7a** was obtained according to the procedure given for the general solution coupling from [1,1′-biphenyl]-4-carboxylic acid and **6a** (Supporting Information). ^{1}H NMR (DMSO-d_6, 600 MHz): 8.03 (d, J = 7.8 Hz, 2H), 7.96 (d, J = 7.8 Hz, 2H), 7.79 (d, J = 8.4 Hz, 2H), 7.71 (m, 5H), 7.49 (m, 2H), 7.42 (t, J_1 = 7.2 Hz, J_2 = 7.8 Hz, 1H), 7.30 (t, J_1 = 7.8 Hz, J_2 = 7.8 Hz, 2H), 7.02 (d, J = 8.4 Hz, 2H), 6.95 (t, J_1 = 7.2 Hz, J_2 = 7.2 Hz, 1H), 5.22 (s, 2H). HRMS calcd for $C_{26}H_{21}NO_4S$, 444.1264 (M + H); found, 444.1274. HPLC purity 99.9%, t_R = 11.84 min.

dx.doi.org/10.1021/jm200826s |*J. Med. Chem.* 2011, 54, 6000–6013

Table 5. Relevance of the 4-(Phenoxymethyl)-benzene Moiety of Compound 7b for the Inhibition of Bcl-x_L and Mcl-1 Binding to a BH3 Peptide

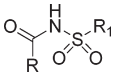

R	R_1	ID	IC_{50} (μM) Bcl-x_L	IC_{50} (μM) Mcl-1
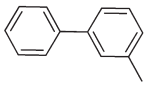	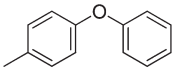	**19**	28.52 ± 0.11	3.24 ± 0.02
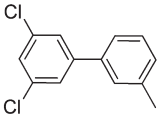	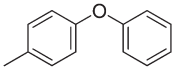	**20**	2.53 ± 0.05	7.11 ± 0.01
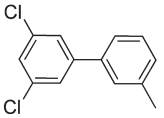	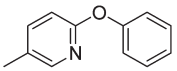	**21**	2.31 ± 0.04	9.78 ± 0.02
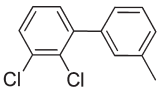	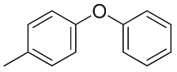	**24**	4.08 ± 0.02	4.76 ± 0.01
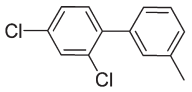	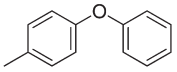	**22**	1.94 ± 0.02	3.72 ± 0.02
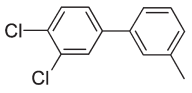	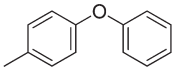	**23**	1.97 ± 0.05	2.48 ± 0.03
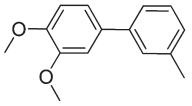	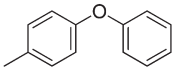	**25**	>1000	42.59 ± 0.06

***N*-((4-(Phenoxymethyl)phenyl)sulfonyl)-[1,1′-biphenyl]-3-carboxamide (7b).** Compound **7b** was obtained according to the procedure given for the general solution coupling from [1,1′-biphenyl]-3-carboxylic acid and **6a** (Supporting Information). ^{1}H NMR (DMSO-d_6, 600 MHz): 8.21 (s, 1H), 8.04 (d, J = 7.8 Hz, 2H), 7.93 (d, J = 7.2 Hz, 1H), 7.82 (d, J = 7.8 Hz, 1H), 7.76 (d, J = 7.8 Hz, 2H), 7.71 (d, J = 8.4 Hz, 2H), 7.58 (s, J_1 = 7.8 Hz, J_2 = 7.2 Hz, 1H), 7.50 (t, J_1 = 7.8 Hz, J_2 = 7.2 Hz, 2H), 7.41 (t, J_1 =7.8 Hz, J_2 = 6.6 Hz, 1H), 7.30 (t, J_1 =7.8 Hz, J_2 = 7.2 Hz, 2H), 7.01 (d, J = 8.4 Hz, 2H), 6.95 (t, J_1 = 7.2 Hz, J_2 = 7.2 Hz, 1H), 5.22 (s, 2H). HRMS calcd for $C_{26}H_{21}NO_4S$, 444.1264 (M + H); found, 444.1280. HPLC purity 99.0%, t_R = 11.67 min.

***N*-((4-(Phenoxymethyl)phenyl)sulfonyl)-[1,1′-biphenyl]-2-carboxamide (7c).** Compound **7c** was obtained according to the procedure given for the general solution coupling from [1,1′-biphenyl]-2-carboxylic acid and **6a** (Supporting Information). ^{1}H NMR (DMSO-d_6, 600 MHz): 7.85 (d, J = 8.4 Hz, 2H), 7.69 (d, J = 7.8 Hz, 2H), 7.56 (t, J_1 =7.8 Hz, J_2 = 7.2 Hz, 1H), 7.49 (d, J = 7.2 Hz, 1H), 7.44 (t, J_1 =7.8 Hz, J_2 = 7.2 Hz, 1H), 7.39 (d, J = 7.8 Hz, 1H), 7.33 (t, J_1 =7.8 Hz, J_2 = 7.8 Hz, 2H), 7.18 (t, J_1 = 6.6 Hz, J_2 = 7.2 Hz, 1H), 7.09−7.04 (m, 7H), 6.98 (t, J_1 = 7.2 Hz, J_2 = 7.3 Hz, 1H), 5.28 (s, 2H). HRMS calcd for $C_{26}H_{21}NO_4S$, 444.1264 (M + H); found, 444.1275. HPLC purity 99.1%, t_R = 10.2 min.

4′-Fluoro-*N*-((4-(phenoxymethyl)phenyl)sulfonyl)-[1,1′-biphenyl]-4-carboxamide (8). Compound **8** was obtained according to the procedure given for the general solution coupling from 4′-fluoro-[1,1′-biphenyl]-4-carboxylic acid and **6a** (Supporting Information). ^{1}H NMR (DMSO-d_6, 600 MHz): 8.03 (d, J = 8.4 Hz, 2H), 7.95 (d, J = 8.4 Hz, 2H), 7.80−7.77 (m, 5H), 7.70 (d, J = 8.4 Hz, 2H), 7.33−7.29 (m, 4H), 7.02 (d, J = 8.4 Hz, 2H), 6.95 (t, J_1 = 7.2 Hz, J_2 = 7.2 Hz, 1H), 5.22 (s, 2H). HRMS calcd for $C_{26}H_{20}FNO_4S$, 462.1170 (M + H); found, 462.1186. HPLC purity 98.9%, t_R = 11.63 min.

4′-Chloro-*N*-((4-(phenoxymethyl)phenyl)sulfonyl)-[1,1′-biphenyl]-4-carboxamide (9). Compound **9** was obtained according to the procedure given for the general solution coupling from 4′-chloro-[1,1′-biphenyl]-4-carboxylic acid and **6a** (Supporting Information). ^{1}H NMR (DMSO-d_6, 600 MHz): 8.02 (d, J = 7.8 Hz, 2H), 7.96 (d, J = 8.4 Hz, 2H), 7.80 (d, J = 8.4 Hz, 2H), 7.77 (d, J = 7.8 Hz, 2H), 7.70 (d, J = 7.8 Hz, 2H), 7.55 (d, J = 8.4 Hz, 2H), 7.30 (t, J_1 = 7.8 Hz, J_2 = 7.2 Hz, 2H), 7.02 (d, J = 7.8 Hz, 2H), 6.95 (t, J_1 = 7.2 Hz, J_2 = 7.2 Hz, 1H), 5.22 (s, 2H). HRMS calcd for $C_{26}H_{20}ClNO_4S$, 478.0874 (M + H); found, 478.0873. HPLC purity 98.0%, t_R = 13.12 min.

3′,5′-Dichloro-*N*-((4-(phenoxymethyl)phenyl)sulfonyl)-[1,1′-biphenyl]-4-carboxamide (10). Compound **10** was obtained according to the procedure given for the general solution coupling from 3′,5′-dichloro-[1,1′-biphenyl]-4-carboxylic acid and **6a** (Supporting Information). ^{1}H NMR (DMSO-d_6, 600 MHz): 8.04 (d, J = 8.4 Hz, 2H), 7.96 (d, J = 8.4 Hz, 2H), 7.88 (d, J = 8.4 Hz, 2H), 7.82 (s, 2H), 7.70 (d, J = 7.8 Hz, 2H), 7.66 (s, 1H), 7.55 (d, J = 8.4 Hz, 2H), 7.30 (t, J_1 =7.2 Hz, J_2 =

dx.doi.org/10.1021/jm200826s |*J. Med. Chem.* 2011, 54, 6000–6013

Table 6. SAR around the 4-(Phenoxymethyl)-benzene Moiety of Compound 23 for the Affinity to Bcl-x_L and Mcl-1

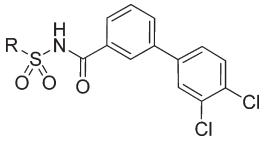

R	ID	IC_{50} (μM) Bcl-x_L	IC_{50} (μM) Mcl-1
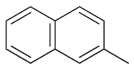	**26**	10.87 ± 0.11	13.20 ± 0.91
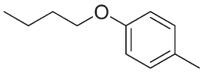	**27**	12.11 ± 0.02	38.81 ± 0.21
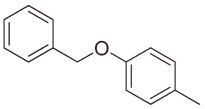	**28**	2.96 ± 0.02	4.88 ± 0.02
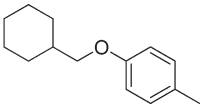	**29**	0.16 ± 0.16	0.62 ± 0.21
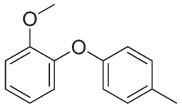	**30**	3.76 ± 0.03	6.63 ± 0.02
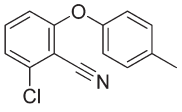	**31**	2.70 ± 0.03	3.18 ± 0.01
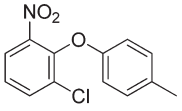	**32**	2.00 ± 0.04	3.04 ± 0.01
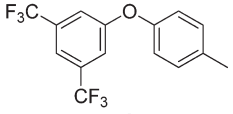	**33**	2.94 ± 0.89	3.04 ± 0.01
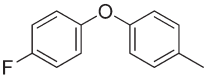	**34**	2.87 ± 0.03	3.91 ± 0.02
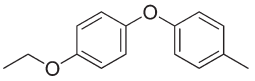	**35**	0.086 ± 0.21	0.14 ± 0.07

7.8 Hz, 2H), 7.02 (d, J = 8.4 Hz, 2H), 6.95 (t, J_1 =7.2 Hz, J_2 = 7.2 Hz, 1H), 5.23 (s, 2H). HRMS calcd for $C_{26}H_{19}Cl_2NO_4S$, 512.0485 (M + H); found, 512.0483. HPLC purity 99.1%, t_R = 14.77 min.

***N*-((4-Phenoxyphenyl)sulfonyl)-[1,1′-biphenyl]-4-carboxamide (11).** Compound **11** was obtained according to the procedure given for the general solution coupling (Figure 2C) from [1,1′-biphenyl]-4-carboxylic acid and **6b** (Supporting Information). ^{1}H NMR (DMSO-d_6, 600 MHz): 8.00 (d, J = 9.0 Hz, 2H), 7.96 (d, J = 8.4 Hz, 2H), 7.80 (d, J = 7.8 Hz, 2H), 7.73 (d, J = 7.2 Hz, 2H), 7.51−7.46 (m, 4H), 7.42 (t, J_1 = 7.2 Hz, J_2 = 7.2 Hz, 1H), 7.27 (t, J_1 = 7.2 Hz, J_2 = 7.2 Hz, 1H), 7.17−7.14 (m, 4H). HRMS calcd for $C_{25}H_{19}NO_4S$, 430.1107 (M + H); found, 430.1124. HPLC purity 99.0%, t_R = 11.70 min.

4′-Fluoro-*N*-((4-phenoxyphenyl)sulfonyl)-[1,1′-biphenyl]-4-carboxamide (12). Compound **12** was obtained according to the procedure given for the general solution coupling from 4′-fluoro-[1,1′-biphenyl]-4-carboxylic acid and **6b** (Supporting Information). ^{1}H NMR (DMSO-d_6, 600 MHz): 8.0 (d, J = 8.4 Hz, 2H), 7.95 (d, J = 7.8 Hz, 2H), 7.78−7.73 (m, 5H), 7.47 (t, J_1 = 7.8 Hz, J_2 = 7.2 Hz, 2H), 7.32 (t, J_1 = 8.4 Hz, J_2 = 8.4 Hz, 2H), 7.28−7.26 (m, 1H), 7.17−7.13 (m, 4H). HRMS calcd for $C_{25}H_{18}FNO_4S$, 448.1013 (M + H); found, 448.1018. HPLC purity 97.2%, t_R = 11.74 min.

3′,5′-Dichloro-*N*-((4-phenoxyphenyl)sulfonyl)-[1,1′-biphenyl]-4-carboxamide (13). Compound **13** was obtained according to the procedure given for the general solution coupling from 3′,5′-dichloro-[1,1′-biphenyl]-4-carboxylic acid and **6b** (Supporting Information). ^{1}H NMR (DMSO-d_6, 600 MHz): 8.0 (d, J = 9 Hz, 2H), 7.97 (d, J = 8.4 Hz, 2H), 7.89−7.86 (m, 3H), 7.82 (s, 2H), 7.66 (s, 1H), 7.47 (t, J_1 = 7.8 Hz, J_2 7.8 Hz, 2H), 7.27 (t, J_1 = 7.2 Hz, J_2 = 7.2 Hz, 1H), 7.17−7.13 (m, 4H). HRMS calcd for $C_{25}H_{17}Cl_2NO_4S$, 498.0328 (M + H); found, 498.0331. HPLC purity >99.9%, t_R = 15.10 min.

***N*-((4-(Benzyloxy)phenyl)sulfonyl)-3′,5′-dichloro-[1,1′-biphenyl]-4-carboxamide (13a).** Compound **13a** was obtained according to the procedure given for the general solution coupling from 3′,5′-dichloro-[1,1′-biphenyl]-4-carboxylic acid and 4-(benzyloxy)-

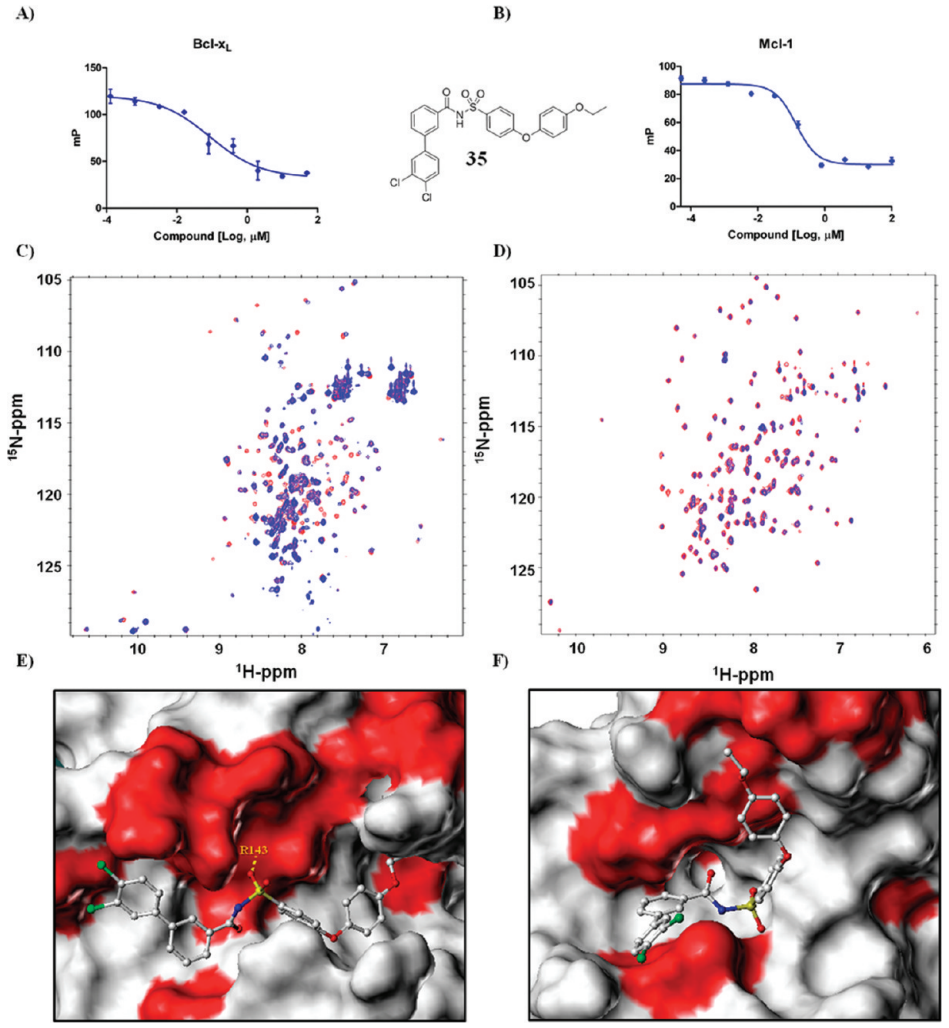

Figure 5. Binding affinity and chemical shift mapping studies of compound **35** with Bcl-x_L and Mcl-1. FPA displacement curves against Bcl-x_L (A), Mcl-1 (B), and chemical structure of compound **35**. [^{15}N, ^{1}H]-HSQC spectra of Bcl-x_L (C) and Mcl-1 (D) in the absence (red) and presence (blue) of compound **35** 1:1 molar ratio. Docked structure of compound **35** is reported into the BH3-binding pocket of Bcl-x_L (PDB ID 1YSI) (E), and into the BH3-binding pocket of Mcl-1 (PDB ID 2NL9) (F). The MOLCAD protein surfaces are colored according to the chemical shift perturbations (red, residues with $\Delta\delta \geq 0.1$ ppm upon complexation).

benzenesulfonamide. ^{1}H NMR (DMSO-d_6, 600 MHz): 12.53 (s, 1H), 7.95 (m, 4H), 7.89 (d, J = 8.1 Hz, 2H), 7.83 (s, 2H), 7.67 (s, 1H), 7.47 (d, J = 7.4 Hz, 2H), 7.41 (m, 2H), 7.36 (m, 1H), 7.24 (d, J = 8.5 Hz, 2H), 5.21 (s, 2H). MS calcd for $C_{26}H_{19}Cl_2NO_4S$, 511.0412; found, 511.85 (Supporting Information).

***N*-([1,1′-Biphenyl]-4-ylsulfonyl)-4-phenoxybenzamide (14).** Compound **14** was obtained according to the procedure given for the general solution coupling from 4-phenoxybenzoic acid and **6c** (Supporting Information). ^{1}H NMR (DMSO-d_6, 600 MHz): 8.06 (d, J = 7.8 Hz, 2H), 7.92 (m, 5H), 7.74 (d, J = 7.2 Hz, 2H), 7.52 (t, J_1 = 7.2 Hz, J_2 = 7.2 Hz, 2H), 7.49 (t, J_1 = 6.6 Hz, J_2 = 7.2 Hz, 3H), 7.24 (t, J_1 = 6.6 Hz, J_2 = 7.2 Hz, 1H), 7.10 (d, J = 7.8 Hz, 2H), 7.01 (d, J = 8.4 Hz, 2H). HRMS calcd for $C_{25}H_{19}NO_4S$, 430.1107 (M + H); found, 430.1128. HPLC purity 99.0%, t_R = 11.52 min.

***N*-((4-(Phenoxymethyl)phenyl)sulfonyl)-4′-(trifluoromethyl)-[1,1′-biphenyl]-3-carboxamide (15).** Compound **15** was obtained according to the procedure given for the general solution coupling from 4′-(trifluoromethyl)-[1,1′-biphenyl]-3-carboxylic acid and **6a** (Supporting Information). ^{1}H NMR (DMSO-d_6, 600 MHz): 8.27 (s, 1H), 8.04 (d, J = 8.4 Hz, 2H), 7.99 (d, J = 7.8 Hz, 3H), 7.89 (d, J = 7.8 Hz, 1H), 7.86 (d, J = 7.8 Hz, 2H), 7.69 (d, J = 8.4 Hz, 2H), 7.62 (t, J_1 = 7.8 Hz, J_2 = 7.8 Hz, 1H), 7.29 (t, J_1 = 7.8 Hz, J_2 = 7.8 Hz, 2H), 7.01 (d, J = 7.8 Hz, 2H), 6.95 (t, J_1 = 7.2 Hz, J_2 = 7.2 Hz, 1H), 5.22 (s, 2H). HRMS calcd for $C_{27}H_{20}F_3NO_4S$, 512.1138 (M + H); found, 512.1145. HPLC purity 99.9%, t_R = 13.43 min.

3′,5′-Dichloro-*N*-((4-(phenoxymethyl)phenyl)sulfonyl)-[1,1′-biphenyl]-3-carboxamide (16). Compound **16** was obtained according to the procedure given for the general solution coupling from 3′,5′-dichloro-[1,1′-biphenyl]-3-carboxylic acid and **6a** (Supporting Information). ^{1}H NMR (DMSO-d_6, 600 MHz): 8.24 (s, 1H), 8.04 (d, J = 7.8 Hz, 2H), 8.0 (d, J = 7.2 Hz, 1H), 7.87 (s, 1H), 7.85 (s, 2H), 7.70 (d, J = 7.8 Hz, 2H), 7.65 (s, 1H), 7.59 (t, J_1 = 7.8 Hz, J_2 = 7.8 Hz, 1H), 7.30 (t, J_1 = 7.2 Hz, J_2 = 7.8 Hz, 2H), 7.02 (d, J = 8.4 Hz, 2H) 6.95 (t, J_1 = 7.2 Hz, J_2 = 7.2 Hz, 1H), 5.22 (s, 2H). HRMS calcd for $C_{26}H_{19}Cl_2NO_4S$, 534.0304 (M + Na); found, 534.0303. HPLC purity 99.4%, t_R = 14.94 min.

***N*-((4-(Benzyloxy)phenyl)sulfonyl)-3′,5′-dichloro-[1,1′-biphenyl]-3-carboxamide (16a).** Compound **16a** was obtained according to the procedure given for the general solution coupling from 3′,5′-dichloro-[1,1′-biphenyl]-3-carboxylic acid and 4-(benzyloxy)benzenesulfonamide (Supporting Information). ^{1}H NMR (DMSO-d_6, 600 MHz): 8.22 (s, 1H), 8.01 (m, 2H), 7.96 (d, J = 10.8 Hz, 2H), 7.86 (s, 2H), 7.79 (s, 1H), 7.65 (s, 1H), 7.59 (t, J_1 = 7.8 Hz, J_2 = 7.2 Hz, 1H), 7.46 (d, J = 7.2 Hz,2H), 7.40 (t, J_1 = 6.6 Hz, J_2 = 7.2 Hz, 2H), 7.23 (d, J = 7.8

dx.doi.org/10.1021/jm200826s |*J. Med. Chem.* 2011, 54, 6000–6013

Hz, 2H), 5.21 (s, 2H). MS calcd for $C_{26}H_{19}Cl_2NO_4S$, 511.0412; found, 511.90, (Supporting Information).

2′,4′-Dichloro-*N*-((4-(phenoxymethyl)phenyl)sulfonyl)-[1,1′-biphenyl]-3-carboxamide (17). Compound **17** was obtained according to the procedure given for the general solution coupling from 2′,4′-dichloro-[1,1′-biphenyl]-3-carboxylic acid and **6a** (Supporting Information). ^{1}H NMR (DMSO-d_6, 600 MHz): 8.01 (d, J = 6.6 Hz, 2H), 7.92−7.90 (m, 3H), 7.76 (s, 1H), 7.68 (m, 3H), 7.58−7.54 (m, 2H), 7.50 (d, J = 8.4 Hz, 1H), 7.29 (t, J_1 = 7.2 Hz, J_2 = 7.8 Hz, 2H), 7.01 (d, J = 7.8 Hz, 2H), 6.94 (t, J_1 = 7.2 Hz, J_2 = 7.8 Hz, 1H), 5.21 (s, 2H). HRMS calcd for $C_{26}H_{19}Cl_2NO_4S$, 534.0304 (M + Na); found, 534.0303. HPLC purity 99.0%, t_R = 14.34 min.

3′,4′-Dichloro-*N*-((4-(phenoxymethyl)phenyl)sulfonyl)-[1,1′-biphenyl]-3-carboxamide (18). Compound **18** was obtained according to the procedure given for the general solution coupling from 3′,4′-dichloro-[1,1′-biphenyl]-3-carboxylic acid and **6a** (Supporting Information). ^{1}H NMR (DMSO-d_6, 600 MHz): 8.17 (s, 1H), 7.92−7.88 (m, 4H), 7.76 (m, 1H), 7.71 (d, J = 8.4 Hz, 1H), 7.67 (d, J = 8.4 Hz, 1H), 7.51 (m, 2H), 7.46 (m, 1H), 7.28 (t, J_1 = 7.8 Hz, J_2 = 7.8 Hz, 2H), 7.0 (d, J = 7.8 Hz, 2H), 6.93 (t, J_1 = 6.6 Hz, J_2 = 7.8 Hz, 1H), 5.14 (s, 2H). HRMS calcd for $C_{26}H_{19}Cl_2NO_4S$, 534.0304 (M + Na); found, 534.0405. HPLC purity 99.4%, t_R = 14.56 min.

***N*-((4-Phenoxyphenyl)sulfonyl)-[1,1′-biphenyl]-3-carboxamide (19).** Compound **19** was obtained according to the procedure given for the general solution coupling from [1,1′-biphenyl]-3-carboxylic acid and **6b** (Supporting Information). ^{1}H NMR (DMSO-d_6, 600 MHz): 8.20 (s, 1H), 8.01 (d, J = 8.4 Hz, 2H), 7.92 (d, J = 6.6 Hz, 1H), 7.83 (d, J = 7.8 Hz, 1H), 7.75 (d, J = 7.8 Hz, 2H), 7.58 (t, J_1 =7.2 Hz, J_2 = 7.8 Hz, 1H), 7.51−7.46 (m, 4H), 7.42 (m, 1H), 7.27 (m, 1H), 7.17−7.13 (m, 4H). HRMS calcd for $C_{25}H_{19}NO_4S$, 430.1107 (M + H); found, 430.1125. HPLC purity 99.0%, t_R = 11.84 min.

3′,5′-Dichloro-*N*-((4-phenoxyphenyl)sulfonyl)-[1,1′-biphenyl]-3-carboxamide (20). Compound **20** was obtained according to the procedure given for the general solution coupling from 3′,5′-dichloro-[1,1′-biphenyl]-3-carboxylic acid and **6b** (Supporting Information). ^{1}H NMR (DMSO-d_6, 600 MHz): 8.24 (s, 2H), 8.02−8.0 (m, 3H), 7.88−7.84 (m, 3H), 7.66 (s, 1H), 7.60 (t, J_1 = 7.2 Hz, J_2 = 7.8 Hz, 1H), 7.27 (m, 1H), 7.16−7.13 (m, 4H). HRMS calcd for $C_{25}H_{17}Cl_2NO_4S$, 498.0328 (M + H); found, 498.0327. HPLC purity 97.1%, t_R = 15.24 min.

3′,5′-Dichloro-*N*-((6-phenoxypyridin-3-yl)sulfonyl)-[1,1′-biphenyl]-3-carboxamide (21). Compound **21** was obtained according to the procedure given for the general solution coupling from 3′,5′-dichloro-[1,1′-biphenyl]-3-carboxylic acid and **6b** (Supporting Information). ^{1}H NMR (DMSO-d_6, 600 MHz): 8.60 (bs, 1H), 8.30 (bs, 1H), 8.20 (s, 1H), 7.92 (d, J = 7.2 Hz, 1H), 7.86 (bs, 1H), 7.56 (m, 2H), 7.62 (s, 1H), 7.27 (m, 1H), 7.51 (bs, 1H), 7.44 (m, 2H), 7.25 (t, J_1 = 7.2 Hz, J_2 = 7.2 Hz, 1H), 7.18 (d, J = 7.2 Hz, 2H), 7.11 (bs, 1H). HRMS calcd for $C_{24}H_{16}Cl_2N_2O_4S$, 499.0281 (M + H); found, 499.0285. HPLC purity 95.4%, t_R = 14.31 min.

2′,4′-Dichloro-*N*-((4-phenoxyphenyl)sulfonyl)-[1,1′-biphenyl]-3-carboxamide (22). Compound **22** was obtained according to the procedure given for the general solution coupling from 2′,4′-dichloro-[1,1′-biphenyl]-3-carboxylic acid and **6b** (Supporting Information). ^{1}H NMR (DMSO-d_6, 600 MHz): 7.99 (d, J = 8.4 Hz, 2H), 7.93−7.91 (m, 3H), 7.77 (s, 1H), 7.71 (d, J = 7.2 Hz, 1H), 7.59 (t, J_1 = 7.8 Hz, J_2 = 7.2 Hz, 1H), 7.55 (d, J = 7.8 Hz, 1H), 7.51 (d, J = 8.4 Hz, 1H), 7.47(t, J_1 = 7.8 Hz, J_2 = 7.2 Hz, 2H), 7.27(t, J_1 = 7.8 Hz, J_2 = 7.2 Hz, 1H), 7.16−7.12 (m, 4H). HRMS calcd for $C_{25}H_{17}Cl_2NO_4S$, 498.0328 (M + H); found, 498.0351. HPLC purity 99.0%, t_R = 14.56 min.

3′,4′-Dichloro-*N*-((4-phenoxyphenyl)sulfonyl)-[1,1′-biphenyl]-3-carboxamide (23). Compound **23** was obtained according to the procedure given for the general solution coupling from 3′,4′-dichloro-[1,1′-biphenyl]-3-carboxylic acid and **6b** (Supporting Information). ^{1}H NMR (DMSO-d_6, 600 MHz): 8.23 (s, 2H), 8.06 (s, 1H), 8.01 (d, J = 8.4 Hz, 2H), 7.98 (d, J = 7.8 Hz, 1H), 7.86 (d, J = 7.8 Hz, 1H), 7.78−7.75 (m, 2H), 7.59 (t, J_1 = 7.2 Hz, J_2 = 7.8 Hz, 1H), 7.47 (t, J_1 = 7.8 Hz, J_2 = 7.2 Hz, 2H), 7.27 (t, J_1 = 7.8 Hz, J_2 = 7.2 Hz, 1H), 7.16−7.13 (m, 4H). HRMS calcd for $C_{25}H_{17}Cl_2NO_4S$, 498.0328 (M + H); found, 498.0317. HPLC purity 99.3%, t_R = 14.84 min.

2′,3′-Dichloro-*N*-((4-phenoxyphenyl)sulfonyl)-[1,1′-biphenyl]-3-carboxamide (24). Compound **24** was obtained according to the procedure given for the general solution coupling from 2′,3′-dichloro-[1,1′-biphenyl]-3-carboxylic acid and **6b** (Supporting Information). ^{1}H NMR (DMSO-d_6, 600 MHz): 7.98 (d, J = 7.8 Hz, 2H), 7.94−7.92 (m, 3H), 7.70 (d, J = 7.8 Hz, 2H), 7.56 (m, 1H), 7.47 (t, J_1 = 7.2 Hz, J_2 = 7.8 Hz, 3H), 7.42 (d, J = 7.8 Hz, 1H), 7.26 (m, 1H), 7.15 (d, J = 7.8 Hz, 2H), 7.12 (d, J = 7.8 Hz, 2H). HRMS calcd for $C_{25}H_{17}Cl_2NO_4S$, 498.0328 (M + H); found, 498.0336. HPLC purity 98.3%, t_R = 13.83 min.

3′,4′-Dimethoxy-*N*-((4-phenoxyphenyl)sulfonyl)-[1,1′-biphenyl]-3-carboxamide (25). Compound **25** was obtained according to the procedure given for the general solution coupling from 3′,4′-dimethoxy-[1,1′-biphenyl]-3-carboxylic acid and **6b** (Supporting Information). ^{1}H NMR (DMSO-d_6, 600 MHz): 8.12 (s, 2H), 8.01 (d, J = 8.4 Hz, 2H), 7.90 (d, J = 7.2 Hz, 1H), 7.78 (d, J = 7.8 Hz, 1H), 7.54 (t, J_1 = 7.2 Hz, J_2 = 7.8 Hz, 1H), 7.47 (t, J_1 = 7.8 Hz, J_2 = 7.2 Hz, 2H), 7.28 (m 3H), 7.15 (m, 3H), 7.06 (d, J = 7.8 Hz, 1H), 3.85 (s, 3H), 3.80 (s, 3H). HRMS calcd for $C_{27}H_{23}NO_6S$, 490.1319 (M + H); found, 490.1332. HPLC purity 99.7%, t_R = 10.27 min.

3′,4′-Dichloro-*N*-(naphthalen-2-ylsulfonyl)-[1,1′-biphenyl]-3-carboxamide (26). Compound **26** was obtained according to the procedure given for the general solution coupling from 3′,4′-dichloro-[1,1′-biphenyl]-3-carboxylic acid and naphthalene-2-sulfonamide. ^{1}H NMR (DMSO-d_6, 600 MHz): 8.71 (s, 1H), 8.25 (m, 2H), 8.16 (d, J = 8.4 Hz, 1H), 8.06 (m, 2H), 7.98 (m, 2H), 7.83 (d, J = 7.8 Hz, 1H), 7.75 (m, 4H), 7.70 (t, J_1 = 7.8 Hz, J_2 = 7.2 Hz, 1H), 7.57 (t, J_1 = 7.8 Hz, J_2 = 7.2 Hz, 1H). MS calcd for $C_{23}H_{15}Cl_2NO_3S$, 455.0150; found, 455.90 (Supporting Information).

***N*-((4-Butoxyphenyl)sulfonyl)-3′,4′-dichloro-[1,1′-biphenyl]-3-carboxamide (27).** Compound **27** was obtained according to the procedure given for the general solution coupling from 3′,4′-dichloro-[1,1′-biphenyl]-3-carboxylic acid and 4-butoxybenzenesulfonamide. ^{1}H NMR (DMSO-d_6, 600 MHz): 8.19 (s, 1H), 7.97 (m, 3H), 7.73 (m, 3H), 7.72 (d, J = 7.8 Hz, 2H), 7.61 (t, J_1 = 7.8 Hz, J_2 = 7.8 Hz, 1H), 7.06 (d, J = 7.8 Hz, 2H), 4.03 (t, J_1 = 6.0 Hz, J_2 = 6.0 Hz, 2H), 1.69 (m, 2H), 1.42 (m, 2H), 0.92 (t, J_1 = 7.2 Hz, J_2 = 7.2 Hz, 3H). MS calcd for $C_{23}H_{21}Cl_2NO_4S$, 477.0568; found, 477.90 (Supporting Information).

***N*-((4-(Benzyloxy)phenyl)sulfonyl)-3′,4′-dichloro-[1,1′-biphenyl]-3-carboxamide (28).** Compound **28** was obtained according to the procedure given for the general solution coupling from 3′,4′-dichloro-[1,1′-biphenyl]-3-carboxylic acid and 4 (benzyloxy)benzenesulfonamide. ^{1}H NMR (DMSO-d_6, 600 MHz): 12.51 (s, 1H), 8.22 (s, 1H), 8.06 (s, 1H), 7.95 (m, 3H), 7.84 (d, J = 7.8 Hz, 1H), 7.76 (m, 2H), 7.58 (m, 1H), 7.46 (d, J = 7.2 Hz, 2H), 7.40 (t, J_1 = 7.2 Hz, J_2 = 7.2 Hz, 2H), 7.34 (m, 1H), 7.23 (d, J = 7.8 Hz, 2H), 5.21 (s, 2H). MS calcd for $C_{26}H_{19}Cl_2NO_4S$, 511.0412; found, 511.85 (Supporting Information).

3′,4′-Dichloro-*N*-((4-(cyclohexylmethoxy)phenyl)sulfonyl)-[1,1′-biphenyl]-3-carboxamide (29). Compound **29** was obtained according to the procedure given for the general solution coupling from 3′,4′-dichloro-[1,1′-biphenyl]-3-carboxylic acid and 4-(cyclohexylmethoxy)-benzenesulfonamide. ^{1}H NMR (DMSO-d_6, 600 MHz): 12.53 (s, 1H), 8.21 (s, 1H), 8.06 (s, 1H), 7.97 (d, J = 7.2 Hz, 1H), 7.93 (d, J = 8.4 Hz, 2H), 7.84 (d, J = 7.2 Hz, 1H), 7.76 (m, 2H), 7.58 (t, J_1 = 7.8 Hz, J_2 = 7.2 Hz, 1H), 7.13 (d, J = 8.4 Hz, 2H), 3.88 (d, J = 6.0 Hz, 2H), 1.75 (m, 4H), 1.64 (d, J = 12.0 Hz, 1H), 1.20 (m, 4H), 1.03 (m, 2H). MS calcd for $C_{26}H_{25}Cl_2NO_4S$, 517.0881; found, 517.90 (Supporting Information).

3′,4′-Dichloro-*N*-((4-(2-methoxyphenoxy)phenyl)sulfonyl)-[1,1′-biphenyl]-3-carboxamide (30). Compound **30** was obtained according to the procedure given for the general solution coupling from 3′,4′-dichloro-[1,1′-biphenyl]-3-carboxylic acid and **6c** (Supporting Information). ^{1}H NMR (DMSO-d_6, 600 MHz): 8.15 (s, 1H), 7.92 (d, J = 7.8 Hz, 1H), 7.87 (s, 1H), 7.76 (d, J = 9.0 Hz, 2H), 7.69 (m, 2H), 7.64 (d, J = 7.8 Hz, 1H), 7.41 (t, J_1 = 7.8 Hz, J_2 = 7.8 Hz, 1H), 7.23 (t, J_1 = 7.8 Hz, J_2 = 7.8 Hz, 1H), 7.18 (d, J = 8.4 Hz, 1H), 7.08 (d, J = 7.8 Hz, 1H), 6.98 (t, J_1 = 7.8 Hz, J_2 = 7.2 Hz, 1H), 6.76 (d, J = 8.4 Hz, 2H), 3.73 (s, 3H). HRMS calcd for $C_{27}H_{23}NO_6S$, 528.0434 (M + H); found, 528.0410. HPLC purity 99.5%, t_R = 14.03 min.

3′,4′-Dichloro-*N*-((4-(3-chloro-2-cyanophenoxy)phenyl)-sulfonyl)-[1,1′-biphenyl]-3-carboxamide (31). Compound **31** was obtained according to the procedure given for the general solution coupling from 3′,4′-dichloro-[1,1′-biphenyl]-3-carboxylic acid and 4-(3-chloro-2-cyanophenoxy)benzenesulfonamide. ^{1}H NMR (DMSO-d_6, 600 MHz): 8.23 (s, 1H), 8.08 (d, J = 8.4 Hz, 2H), 8.05 (s, 1H), 7.97 (d, J = 7.8 Hz, 1H), 7.86 (d, J = 7.8 Hz, 1H), 7.74 (m, 4H), 7.58 (m, 2H), 7.38 (d, J = 8.4 Hz, 2H), 7.21 (d, J = 8.4 Hz, 1H). MS calcd for $C_{26}H_{15}Cl_3N_2O_4S$, 555.9818; found, 556.75 (Supporting Information).

3′,4′-Dichloro-*N*-((4-(2-chloro-6-nitrophenoxy)phenyl)-sulfonyl)-[1,1′-biphenyl]-3-carboxamide (32). Compound **32** was obtained according to the procedure given for the general solution coupling from 3′,4′-dichloro-[1,1′-biphenyl]-3-carboxylic acid and 4-(2-chloro-6-nitrophenoxy)benzenesulfonamide. ^{1}H NMR (DMSO-d_6, 600 MHz): 8.23 (s, 1H), 8.17 (d, J = 7.8 Hz, 1H), 8.06 (m, 3H), 8.02 (d, J = 8.4 Hz, 2H), 7.97 (d, J = 7.8 Hz, 1H), 7.86 (d, J = 7.8 Hz, 1H), 7.75 (m, 2H), 7.64 (t, J_1 = 8.4 Hz, J_2 = 7.8 Hz, 1H), 7.59 (t, J_1 = 7.8 Hz, J_2 = 7.8 Hz, 1H), 7.15 (d, J = 8.4 Hz, 2H). MS calcd for $C_{25}H_{15}Cl_3N_2O_6S$, 575.9716; found, 576.70 (Supporting Information).

***N*-((4-(3,5-Bis(trifluoromethyl)phenoxy)phenyl)sulfonyl)-3′,4′-dichloro-[1,1′-biphenyl]-3 carboxamide (33).** Compound **33** was obtained according to the procedure given for the general solution coupling from 3′,4′-dichloro-[1,1′-biphenyl]-3-carboxylic acid and 4-(3,5-bis(trifluoromethyl)phenoxy)benzenesulfonamide. ^{1}H NMR (DMSO-d_6, 600 MHz): 8.24 (s, 1H), 8.06 (m, 2H), 7.98 (m, 1H), 7.95 (s, 1H), 7.93 (s, 2H), 7.87 (m, 2H), 7.80 (s, 1H), 7.77 (s, 1H), 7.60 (t, J_1 = 7.2 Hz, J_2 = 7.2 Hz, 1H), 7.37 (s, 1H), 7.30 (d, J = 7.8 Hz, 2H). MS calcd for $C_{27}H_{15}Cl_2F_6NO_4S$, 633.0003; found, 633.70 (Supporting Information).

3′,4′-Dichloro-*N*-((4-(4-fluorophenoxy)phenyl)sulfonyl)-[1,1′-biphenyl]-3-carboxamide (34). Compound **34** was obtained according to the procedure given for the general solution coupling from 3′,4′-dichloro-[1,1′-biphenyl]-3-carboxylic acid and 4-(4-fluorophenoxy)benzenesulfonamide. ^{1}H NMR (DMSO-d_6, 600 MHz): 8.23 (s, 1H), 8.06 (s, 1H), 7.99 (m, 4H), 7.86 (d, J = 7.2 Hz, 1H), 7.76 (m, 2H), 7.59 (m, 1H), 7.46 (d, J = 7.2 Hz, 1H), 7.40 (t, 2H), 7.12 (d, J = 7.8 Hz, 2H). MS calcd for $C_{25}H_{16}Cl_2FNO_4S$, 515.0161; found, 515.85 (Supporting Information).

3′,4′-Dichloro-*N*-((4-(4-ethoxyphenoxy)phenyl)sulfonyl)-[1,1′-biphenyl]-3-carboxamide (35). Compound **35** was obtained according to the procedure given for the general solution coupling from 3′,4′-dichloro-[1,1′-biphenyl]-3-carboxylic acid and 4-(4-ethoxyphenoxy)benzenesulfonamide. ^{1}H NMR (DMSO-d_6, 600 MHz): 8.22 (s, 1H), 8.05 (s, 1H), 7.97 (m, 3H), 7.85 (d, J = 7.2 Hz, 1H), 7.76 (m, 2H), 7.59 (m, 1H), 7.09 (d, J = 9.0 Hz, 2H), 7.06 (d, J = 8.4 Hz, 2H), 6.99 (d, J = 8.4 Hz, 2H), 4.02 (m, 2H), 1.32 (t, J_1 = 6.6 Hz, J_2 = 7.2 Hz, 3H). MS calcd for $C_{27}H_{21}Cl_2NO_5S$, 541.0517; found, 542.00 (Supporting Information).

Library Design. The NMR compound library we have assembled is composed by 500 low molecular weight compounds representing diverse core structures. In particular, during the design of the library, special emphasis was put into the chemical properties of the selected compounds in an attempt to address "drug-likeness" on empirical grounds. In addition, the compounds were selected in view of their subsequent use as building blocks for the synthesis of bidentate compounds, thus eliminating fragments that would lead to ligands with undesirable critical properties. To predict favorable outcome in ADME (adsorption, distribution, metabolism, excretion) studies as well as final success as drug in humans, we adopted the criteria summarized as follows: average molecular weight < 300; octanol/water repartition coefficient (LogP) < 1.3; number of rotatable bonds between 0 and 2. Moreover, when selecting the scaffolds, we took in account the availability of each fragment in larger amounts at low cost as well as ease of synthesis and conversion to more complex structures. This library was assembled and individual 1D ^{1}H NMR spectra were measured in D_2O buffer as control of compound purity, stability, and solubility in water buffer.

Molecular Modeling. Molecular modeling studies were conducted on a Linux workstation and a 64 3.2 GHz CPUs Linux cluster. Docking studies were performed using the crystal structure of Bcl-x_L and Mcl-1 in complex with a BH3mimetic ligand (Protein Data Bank codes 2YXJ and 2NL9, respectively).[7,31−33] The ligand was extracted from the protein structure and was used to define the binding site for small molecules. Compounds were docked into the Bcl-2 family protein by the GOLD[27] docking program using GoldScore[28] as the scoring function. The active site radius was set at 10 Å, and 10GA solutions were generated for each molecule. The GA docking procedure in GOLD[27] allowed the small molecules to flexibly explore the best binding conformations, whereas the protein structure was static. The protein surface was prepared with the program MOLCAD[34] as implemented in Sybyl (Tripos, St. Louis, MO) and was used to analyze the binding poses for studied small molecules.

Fluorescence Polarization Assays (FPAs). A Bak BH3 peptide (F-BakBH3) (GQVGRQLAIIGDDINR) was labeled at the N-terminus with fluorescein isothiocyanate (FITC) (Molecular Probes) and purified by HPLC. For competitive binding assays, 100 nM GST−Bcl-X_L ΔTM protein was preincubated with the tested compound at varying concentrations in 47.5 μL PBS (pH = 7.4) in 96-well black plates at room temperature for 10 min, then 2.5 μL of 100 nM FITC-labeled Bak BH3 peptide was added to produce a final volume of 50 μL. The wild-type and mutant Bak BH3 peptides were included in each assay plate as positive and negative controls, respectively. After 30 min incubation at room temperature, the polarization values in millipolarization units[35] were measured at excitation/emission wavelengths of 480/535 nm with a multilabel plate reader (PerkinElmer). IC_{50} was determined by fitting the experimental data to a sigmoidal dose−response nonlinear regression model (SigmaPlot 10.0.1, Systat Software, Inc., San Jose, CA, USA). Data reported are mean of three independent experiments ± standard error (SE). Performance of Mcl-1 FPA is similar. Briefly, 50 nM of GST-Mcl-1 was incubated with various concentrations of compound for 2 min, then 15 nM FITC-conjugated-Bim BH3 peptide[36] was added in PBS buffer. Fluorescence polarization was measured after 10 min.

NMR Experiments and Protein Eexpression. NMR-based binding assays have been conducted by acquiring one-dimensional ^{1}H experiments with 500 μL solution of Bcl-x_L at 20 μM concentration, in the absence and presence of added compounds, each at 200 μM concentrations. By observing the aliphatic region of the spectra, binding could be readily detected due to chemical shift changes in active site methyl groups of Ile, Leu, Thr, Val, or Ala (region between −0.8 and 0.3 ppm).[26] All experiments were performed with a 700 MHz Bruker Avance spectrometer equipped with a cryogenic probe and z-axis pulse-field gradients.

NMR-based screening and general experiments have been conducted by acquiring 2D-NOESY experiments with a 500 μL solution of Bcl-x_L in the absence and presence of added compounds, concentrations were depending on the kind of experiment. For all NMR experiments, Bcl-x_L was exchanged into 50 mM phosphate buffer at pH 7.5 and measurements were performed at 300 °F. 2D [^{1}H, ^{1}H]-NOESY spectra were acquired with small molecules at a concentration of 0.25−1.0 mM in the

presence of 10 μM Bcl-x_L. 2D [^{1}H,^{1}H]-NOESY spectra were typically acquired with 8 scans for each of 400 indirect points, a ^{1}H $\pi/2$ pulse length of 11 μs, sweep widths of 12 ppm in both dimensions, mixing times of 300−800 ms, and a recycle delay of 1 s. In all experiments, dephasing of residual water signals was obtained with a WATERGATE sequence. The binding mode of the compounds has been characterized by recording [^{15}N, ^{1}H]-HSQC experiments with a 500 μL solution of uniformly ^{15}N-labeled Bcl-x_L in the absence and presence of added compounds at indicated concentration. ^{15}N and unlabeled Bcl-x_L samples were prepared and purified as described previously. Briefly, *E. coli* strain BL21 was transformed with the pET-21b plasmid (Novagen) carrying the gene coding for Bcl-x_L ΔTM (Bcl-x_L deletion mutant lacking the transmembrane domain). To obtain ^{15}N labeled protein, bacteria were grown on M9 minimal media supported with 2 g/L of ^{13}C-glucose and/or 0.5 g/L of $^{15}NH_4Cl$. Induction of protein expression was carried out at OD_{600} = 0.6 with 1 mM IPTG for 4 h at 37 °C. Following cell harvest and lysis by sonication, the protein was purified using a Ni-affinity column (Amersham). The eluate was extensively dialyzed against 40 mM phosphate buffer (pH = 7.5) and 150 mM NaCl.

■ ASSOCIATED CONTENT

Supporting Information. Synthetic chemistry and analytical data; dose−response curves; 2D [HSQC] spectra of Bcl-x_L and Mcl-1 in complex with selected compounds. This material is available free of charge via the Internet at http://pubs.acs.org.

■ AUTHOR INFORMATION

Corresponding Author

*Phone: (858) 6463159. Fax: (858) 7955225. E-mail: mpellecchia@sanfordburnham.org.

■ ACKNOWLEDGMENT

We are grateful to the NIH (NCI grant CA149668 to MP) for financial support.

■ ABBREVIATIONS USED

Bcl-2, B-cell lymphoma/leukemia-2; BH3, Bcl-2 homology domain; NMR, nuclear magnetic resonance spectroscopy; SAR, structure−activity relationship; NOESY, nuclear Overhauser effect spectroscopy; ILOE, interligand nuclear Overhauser effect; 1D-^{1}H NMR, one-dimensional ^{1}H nuclear magnetic resonance spectroscopy; HSQC, heteronuclear single quantum correlation; FPA, fluorescence polarization assays; LC-MS, liquid chromatography and tandem mass spectrometry; HPLC, high-performance liquid chromatography; DMSO, dimethyl sulfoxide

■ REFERENCES

(1) Shuker, S. B.; Hajduk, P. J.; Meadows, R. P.; Fesik, S. W. Discovering high-affinity ligands for proteins: SAR by NMR. *Science* **1996**, *274*, 1531–1534.

(2) Hajduk, P. J.; Gerfin, T.; Boehlen, J. M.; Haberli, M.; Marek, D.; Fesik, S. W. High-throughput nuclear magnetic resonance-based screening. *J. Med. Chem.* **1999**, *42*, 2315–2317.

(3) Whitty, A.; Kumaravel, G. Between a rock and a hard place? *Nature Chem. Biol.* **2006**, *2*, 112–118.

(4) Pellecchia, M. Solution nuclear magnetic resonance spectroscopy techniques for probing intermolecular interactions. *Chem. Biol.* **2005**, *12*, 961–971.

(5) Pellecchia, M.; Becattini, B.; Crowell, K. J.; Fattorusso, R.; Forino, M.; Fragai, M.; Jung, D.; Mustelin, T.; Tautz, L. NMR-based techniques in the hit identification and optimization processes. *Expert Opin. Ther. Targets* **2004**, *8*, 597–611.

(6) Petros, A. M.; Dinges, J.; Augeri, D. J.; Baumeister, S. A.; Betebenner, D. A.; Bures, M. G.; Elmore, S. W.; Hajduk, P. J.; Joseph, M. K.; Landis, S. K.; Nettesheim, D. G.; Rosenberg, S. H.; Shen, W.; Thomas, S.; Wang, X.; Zanze, I.; Zhang, H.; Fesik, S. W. Discovery of a potent inhibitor of the antiapoptotic protein Bcl-xL from NMR and parallel synthesis. *J. Med. Chem.* **2006**, *49*, 656–663.

(7) Oltersdorf, T.; Elmore, S. W.; Shoemaker, A. R.; Armstrong, R. C.; Augeri, D. J.; Belli, B. A.; Bruncko, M.; Deckwerth, T. L.; Dinges, J.; Hajduk, P. J.; Joseph, M. K.; Kitada, S.; Korsmeyer, S. J.; Kunzer, A. R.; Letai, A.; Li, C.; Mitten, M. J.; Nettesheim, D. G.; Ng, S.; Nimmer, P. M.; O'Connor, J. M.; Oleksijew, A.; Petros, A. M.; Reed, J. C.; Shen, W.; Tahir, S. K.; Thompson, C. B.; Tomaselli, K. J.; Wang, B.; Wendt, M. D.; Zhang, H.; Fesik, S. W.; Rosenberg, S. H. An inhibitor of Bcl-2 family proteins induces regression of solid tumours. *Nature* **2005**, *435*, 677–681.

(8) Konopleva, M.; Contractor, R.; Tsao, T.; Samudio, I.; Ruvolo, P. P.; Kitada, S.; Deng, X.; Zhai, D.; Shi, Y. X.; Sneed, T.; Verhaegen, M.; Soengas, M.; Ruvolo, V. R.; McQueen, T.; Schober, W. D.; Watt, J. C.; Jiffar, T.; Ling, X.; Marini, F. C.; Harris, D.; Dietrich, M.; Estrov, Z.; McCubrey, J.; May, W. S.; Reed, J. C.; Andreeff, M. Mechanisms of apoptosis sensitivity and resistance to the BH3 mimetic ABT-737 in acute myeloid leukemia. *Cancer Cell* **2006**, *10*, 375–388.

(9) van Delft, M. F.; Wei, A. H.; Mason, K. D.; Vandenberg, C. J.; Chen, L.; Czabotar, P. E.; Willis, S. N.; Scott, C. L.; Day, C. L.; Cory, S.; Adams, J. M.; Roberts, A. W.; Huang, D. C. The BH3 mimetic ABT-737 targets selective Bcl-2 proteins and efficiently induces apoptosis via Bak/Bax if Mcl-1 is neutralized. *Cancer Cell* **2006**, *10*, 389–399.

(10) Del Gaizo Moore, V.; Brown, J. R.; Certo, M.; Love, T. M.; Novina, C. D.; Letai, A. Chronic lymphocytic leukemia requires BCL2 to sequester prodeath BIM, explaining sensitivity to BCL2 antagonist ABT-737. *J. Clin. Invest.* **2007**, *117*, 112–121.

(11) Dash, R.; Azab, B.; Quinn, B. A.; Shen, X.; Wang, X. Y.; Das, S. K.; Rahmani, M.; Wei, J.; Hedvat, M.; Dent, P.; Dmitriev, I. P.; Curiel, D. T.; Grant, S.; Wu, B.; Stebbins, J. L.; Pellecchia, M.; Reed, J. C.; Sarkar, D.; Fisher, P. B. Apogossypol derivative BI-97C1 (Sabutoclax) targeting Mcl-1 sensitizes prostate cancer cells to mda-7/IL-24-mediated toxicity. *Proc. Natl. Acad. Sci. U.S.A* **2011**, *108*, 8785–8790.

(12) Becattini, B.; Pellecchia, M. SAR by ILOEs: An NMR-Based Approach to Reverse Chemical Genetics. *Chemistry* **2006**, *12*, 2658–2662.

(13) Becattini, B.; Sareth, S.; Zhai, D.; Crowell, K. J.; Leone, M.; Reed, J. C.; Pellecchia, M. Targeting apoptosis via chemical design: inhibition of bid-induced cell death by small organic molecules. *Chem. Biol.* **2004**, *11*, 1107–1117.

(14) Becattini, B.; Culmsee, C.; Leone, M.; Zhai, D.; Zhang, X.; Crowell, K. J.; Rega, M. F.; Landshamer, S.; Reed, J. C.; Plesnila, N.; Pellecchia, M. Structure−activity relationships by interligand NOE-based design and synthesis of antiapoptotic compounds targeting Bid. *Proc. Natl. Acad. Sci. U.S.A* **2006**, *103*, 12602–12606.

(15) Fejzo, J.; Lepre, C. A.; Peng, J. W.; Bemis, G. W.; Ajay; Murcko, M. A.; Moore, J. M. The SHAPES strategy: an NMR-based approach for lead generation in drug discovery. *Chem. Biol.* **1999**, *6*, 755–769.

(16) Ni, F. Recent developments in transferred NOEs methods. *Prog. Nucl. Magn. Reson. Spectrosc.* **1994**, *26*, 517–606.

(17) Mayer, M.; Meyer, B. Mapping the active site of angiotensin-converting enzyme by transferred NOE spectroscopy. *J. Med. Chem.* **2000**, *43*, 2093–2099.

(18) Kumar, A.; Ernst, R. R.; Wuthrich, K. A two-dimensional nuclear Overhauser enhancement (2D NOE) experiment for the elucidation of complete proton−proton cross-relaxation networks in biological macromolecules. *Biochem. Biophys. Res. Commun.* **1980**, *95*, 1–6.

(19) Jahnke, W.; Florsheimer, A.; Blommers, M. J.; Paris, C. G.; Heim, J.; Nalin, C. M.; Perez, L. B. Second-site NMR screening and linker design. *Curr. Top. Med. Chem.* **2003**, *3*, 69–80.

(20) Li, D.; DeRose, E. F.; London, R. E. The interligand Overhauser effect: a powerful new NMR approach for mapping structural relationships of macromolecular ligands. *J. Biomol. NMR* **1999**, *15*, 71–76.
(21) Pellecchia, M.; Meininger, D.; Dong, Q.; Chang, E.; Jack, R.; Sem, D. S. NMR-based structural characterization of large protein−ligand interactions. *J. Biomol. NMR* **2002**, *22*, 165–173.
(22) Zerbe, O. *BioNMR in Drug Research*; WILEY-VCH: New York, 2003; pp 439−457.
(23) Kline, A. SAR by NOE? *NMR Newsletter* **1997**, *13*, 472.
(24) Bemis, G. W.; Murcko, M. A. The properties of known drugs. 1. Molecular frameworks. *J. Med. Chem.* **1996**, *39*, 2887–2893.
(25) Becattini, B.; Pellecchia, M. SAR by ILOEs: an NMR-based approach to reverse chemical genetics. *Chemistry* **2006**, *12*, 2658–2662.
(26) Rega, M. F.; Leone, M.; Jung, D.; Cotton, N. J.; Stebbins, J. L.; Pellecchia, M. Structure-based discovery of a new class of Bcl-xL antagonists. *Bioorg. Chem.* **2007**, *35*, 344–353.
(27) Jones, G.; Willett, P.; Glen, R. C.; Leach, A. R.; Taylor, R. Development and validation of a genetic algorithm for flexible docking. *J. Mol. Biol.* **1997**, *267*, 727–748.
(28) Eldridge, M. D.; Murray, C. W.; Auton, T. R.; Paolini, G. V.; Mee, R. P. Empirical scoring functions: I. The development of a fast empirical scoring function to estimate the binding affinity of ligands in receptor complexes. *J. Comput.-Aided Mol. Des.* **1997**, *11*, 425–445.
(29) Placzek, W. J.; Wei, J.; Kitada, S.; Zhai, D.; Reed, J. C.; Pellecchia, M. A survey of the anti-apoptotic Bcl-2 subfamily expression in cancer types provides a platform to predict the efficacy of Bcl-2 antagonists in cancer therapy. *Cell Death Dis.* **2010**, *1*, e40.
(30) Wei, J.; Stebbins, J. L.; Kitada, S.; Dash, R.; Placzek, W.; Rega, M. F.; Wu, B.; Cellitti, J.; Zhai, D.; Yang, L.; Dahl, R.; Fisher, P. B.; Reed, J. C.; Pellecchia, M. BI-97C1, an optically pure apogossypol derivative as pan-active inhibitor of antiapoptotic B-cell lymphoma/leukemia-2 (Bcl-2) family proteins. *J. Med. Chem.* **2010**, *53*, 4166–4176.
(31) Lee, E. F.; Czabotar, P. E.; Smith, B. J.; Deshayes, K.; Zobel, K.; Colman, P. M.; Fairlie, W. D. Crystal structure of ABT-737 complexed with Bcl-xL: implications for selectivity of antagonists of the Bcl-2 family. *Cell Death Differ.* **2007**, *14*, 1711–1713.
(32) Bruncko, M.; Oost, T. K.; Belli, B. A.; Ding, H.; Joseph, M. K.; Kunzer, A.; Martineau, D.; McClellan, W. J.; Mitten, M.; Ng, S. C.; Nimmer, P. M.; Oltersdorf, T.; Park, C. M.; Petros, A. M.; Shoemaker, A. R.; Song, X.; Wang, X.; Wendt, M. D.; Zhang, H.; Fesik, S. W.; Rosenberg, S. H.; Elmore, S. W. Studies leading to potent, dual inhibitors of Bcl-2 and Bcl-xL. *J. Med. Chem.* **2007**, *50*, 641–662.
(33) Czabotar, P. E.; Lee, E. F.; van Delft, M. F.; Day, C. L.; Smith, B. J.; Huang, D. C.; Fairlie, W. D.; Hinds, M. G.; Colman, P. M. Structural insights into the degradation of Mcl-1 induced by BH3 domains. *Proc. Natl. Acad. Sci. U.S.A.* **2007**, *104*, 6217–6222.
(34) Teschner, M.; Henn, C.; Vollhardt, H.; Reiling, S.; Brickmann, J. Texture mapping: a new tool for molecular graphics. *J. Mol. Graphics* **1994**, *12*, 98–105.
(35) Sattler, M.; Liang, H.; Nettesheim, D.; Meadows, R. P.; Harlan, J. E.; Eberstadt, M.; Yoon, H. S.; Shuker, S. B.; Chang, B. S.; Minn, A. J.; Thompson, C. B.; Fesik, S. W. Structure of Bcl-xL-Bak peptide complex: recognition between regulators of apoptosis. *Science* **1997**, *275*, 983–986.
(36) Ramjaun, A. R.; Tomlinson, S.; Eddaoudi, A.; Downward, J. Upregulation of two BH3-only proteins, Bmf and Bim, during TGF beta-induced apoptosis. *Oncogene* **2007**, *26*, 970–981.